Sound & Vibration 2025, 59(4), 3533.
doi: https://doi.org/10.59400/sv3533

Article

Smart tilted FBG sensors for strain monitoring in wooden beams

Aliya Kalizhanova[1,2], Murat Kunelbayev[1,3,*], Ainur Kozbakova[1,4]

[1] Institute of Information and Computational Technologies CS MSHE RK, Almaty 050010, Kazakhstan

[2] Department of IT Engineering and Artificial Intelligence, Almaty University of Energy and Communications named after G. Daukeyev, Almaty 050013, Kazakhstan

[3] Department of Artificial Intelligence and Big Data, Al-Farabi Kazakh National University, Almaty 050040, Kazakhstan

[4] Department of Information Systems, Almaty Technological University, Almaty 050012, Kazakhstan

*** Corresponding author:** Murat Kunelbayev, murat7508@yandex.kz

CITATION

Kalizhanova A, Kunelbayev M, Kozbakova A. Smart tilted FBG sensors for strain monitoring in wooden beams. Sound & Vibration. 2025; 59(4): 3533. https://doi.org/10.59400/sv3533

ARTICLE INFO

Received: 16 July 2025
Revised: 11 August 2025
Accepted: 23 August 2025
Available online: 30 August 2025

Abstract: This paper reports the design, fabrication, and experimental validation of smart tilted fiber Bragg grating (TFBG) sensors embedded within the internal structure of wooden beams for real-time strain and deflection monitoring. Pine and oak specimens were instrumented with five multiplexed FBGs distributed along the span and tested under a constant end load to capture the strain field during bending. To mitigate temperature-induced bias in the deflection analysis, a dedicated reference FBG was placed in a non-deflecting zone and used to compensate the individual temperature response of each sensing element. The optical transducers were encapsulated in epoxy-impregnated carbon fabric to ensure reliable strain transfer, mechanical protection, and long-term stability without compromising the host material. Wavelength-shift demodulation and in-situ calibration provided separate estimates of strain and temperature, enabling accurate reconstruction of the beam shape. The temperature-compensated measurements showed close agreement with Euler–Bernoulli beam predictions for both wood species, with correlation coefficients exceeding 0.87 across all trials. The sensing system exhibited repeatable behavior and low hysteresis, while the embedded configuration preserved the structural integrity and allowed unobtrusive installation. Overall, the results demonstrate that smart TFBG sensors are a practical and effective solution for embedded structural health monitoring of timber members, offering high accuracy, electromagnetic immunity, and seamless integration into load-bearing components. The approach is readily scalable to multi-sensor arrays and mixed materials, paving the way for continuous monitoring of civil and architectural wooden structures.

Keywords: bragg grid fiber-optic sensors; structural condition monitoring; embedded systems; advanced computing; internet of things; real-time signal processing; low-power data collection

1. Introduction

Mechanical and civil engineering structures are subjected to various loads throughout their service life, so condition assessment is essential. Monitoring and safety control allow early detection of issues that may be missed at the construction stage. As shown by Kinet et al. [1], monitoring critical areas affected by wear and corrosion enables more effective preventive measures because these regions often exhibit degraded mechanical properties. In Hong et al. [2], structural health monitoring (SHM) of bridges and tunnels highlighted the advantages of fiber Bragg grating

(FBG) sensors, which are cost-effective, precise, and highly adaptable; they can be surface-mounted on existing structures or embedded during construction. Studies by Diaz et al. [3] and Broadway et al. [4] indicate that optical sensors, thanks to rich data capabilities, are strong alternatives to conventional electromechanical sensors.

FBG sensors offer compact size, low weight, minimal installation footprint, immunity to electromagnetic interference, corrosion resistance, intrinsic safety in explosive environments, multiplexing capability, and high accuracy. Theodosiou and Kalli [5] showed that the photosensitivity of optical fibers enables inscription of Bragg gratings along the fiber core to selectively reflect specific wavelengths. According to Erdogan [6], an FBG reflects a narrow portion of the input spectrum—its Bragg wavelength. Proper sensor calibration and correlation equations for accurate interpretation are described by Lamberti et al. [7] and Leal-Junior et al. [8]. Bernardini et al. [9] developed algorithms for shape reconstruction from strain/deflection/angle measurements using distributed or quasi-distributed sensors, while Elayaperumal et al. [10] presented shape-recovery methods with electrical strain gauges and fiber-optic systems. Wu et al. [11] emphasized the compactness of optical-fiber sensors and their ability to integrate into host materials without significantly altering structural characteristics. Biazi et al. [12] demonstrated 2D (single-plane) shape reconstruction with FBGs. Yi et al. [13] investigated radially arranged, positionable fibers for 3D reconstruction, including cladding-mode and tilted-FBG configurations reported by Waltermann et al. [14] and Feng et al. [15]. Berthelot [16] developed high-resolution optical reflectometry for shape sensing, particularly in biomedical applications.

Composite materials are formed by combining two or more immiscible components with strong adhesion to achieve enhanced properties, as discussed by Gay et al. [17]. Typically, reinforcing fibers (glass or carbon, short or continuous) are embedded in a thermoplastic or thermosetting matrix that transfers strain, protects against the environment, and preserves shape while allowing some deformation; manufacturing routes range from manual resin impregnation and vacuum molding to modern injection techniques [18]. Marques et al. [19] reviewed embedded optical-fiber sensors in diaphragms for aircraft condition monitoring. Fiber-reinforced polymers (FRPs) have attracted attention for exceptional specific properties and are widely used in transportation and civil engineering; Di Sante [20] notes that composites comprise up to 50% of an aircraft's weight (e.g., Boeing 787). To ensure safety and extend service life, SHM systems are applied, as confirmed by Shivakumar and Emmanwori [21] and Jensen and Pascual [22].

Among fiber-optic sensors, FBGs are widely used owing to high precision and robustness against power-fluctuation effects. They monitor strain, transverse load [23], and acceleration [24], as summarized by Kreuzer [25]. Successful integration of FBGs inscribed in standard single-mode fibers (SMFs) into composites for SHM is documented by Kinet et al. [1], Güemes et al. [26], Sierra-Pérez et al. [27], Lamberti et al. [28], and Szebényi et al. [29]. Applications include hydrogen composite pressure vessels [30, 31], wind-turbine blades and high-speed patrol vessels [32], and aircraft components [33]. Luyckx et al. [34] showed that SMF-FBGs measure longitudinal strain accurately and studied response to transverse loads; under transverse pressure,

birefringence splits the Bragg peak into two orthogonal polarization maxima, although at low forces the spectrum may remain single-peaked, complicating separation of the two wavelengths [33]. Building on this, Luyckx et al. [34] and Singh et al. [35] explored birefringence induced during composite curing to detect multiaxial strain and temperature simultaneously.

Intelligent and reconfigurable technologies in SHM systems

Modern structural condition monitoring (SHM) systems integrated with Internet of Things (IoT) technologies allow for continuous and remote monitoring of various objects, from buildings and bridges to aviation and industrial structures. Thanks to the IoT, such systems provide rapid data collection from sensors and their transfer to cloud storage for subsequent analysis and visualization. FPGAs play an important role in the architecture of such systems, providing high-speed and parallel signal processing from multiple sensors, including fiber-optic arrays (FBG), accelerometers, and strain gauges. The use of FPGAs makes it possible to implement adaptive filtering, calibration and diagnostic algorithms, which significantly increases the measurement accuracy and the system's resistance to interference. Additionally, SHM systems actively use predictive analytics based on artificial intelligence — machine and deep learning models (such as SVM, Random Forest, CNN, and LSTM) are trained on large amounts of historical data and allow predicting potential damage, calculating the remaining life of structures, and optimizing maintenance. Thus, the integration of IoT, FPGA, and AI forms the basis for creating intelligent SHM systems capable of early defect detection, adaptive signal processing, and real-time decision making. Modern structural monitoring (SHM) systems are increasingly using edge computing, a technology that allows processing data at the sensor or embedded device level (for example, microcontrollers and FPGAs), which reduces delays and reduces the amount of information transmitted. At the same time, the role of cybersecurity is increasing: encryption protocols (TLS, MQTT over SSL) and built-in hardware protection are used to protect data. More and more SHM solutions rely on the concept of digital twins — virtual models of structures synchronized with real measurements, as well as sensors with automatic calibration function, ensuring long-term stability. Hybrid wireless networks combining Wi-Fi, LoRa and NB-IoT technologies are used to cover objects with varying degrees of remoteness. In addition, the systems are equipped with adaptive AI models that can adapt to operating conditions, which allows maintaining high accuracy in predicting the technical condition.

In this paper, five FBG sensors are integrated along a pine beam and an oak beam. The sensors evaluate a flexible line that traces the deflection along the entire length of the beam, reproducing the results of load tests. Additionally, a method of temperature compensation for cross-susceptibility was also used.

2. Materials and methods

To experimentally verify the proposed method, a test setup was assembled and trials were conducted on two cantilever beams. Pine and oak beams, each 100 mm long with different geometric characteristics, were used as test materials: the pine beam had a diameter of 16 mm, while the oak beam had a rectangular cross-section of 10×11

mm. These materials were chosen due to their differing elastic moduli (6900 MPa for pine and 13,400 MPa for oak), which allowed assessment of the method's effectiveness under varying stiffness conditions.

Each beam was embedded with five Fiber Bragg Grating (FBG) sensors, evenly distributed along its length. One of the sensors (FBG5) was positioned in the clamped region and served as a reference for compensating temperature deviations, as it was not subjected to mechanical deformation. The remaining sensors (FBG1–FBG5) measured the wavelength shift caused by deformations resulting from the applied load.

To generate and control temperature influence, a Votsch VCL4003 thermal chamber was used, with the beam placed inside. A constant load was applied to the free end of the beam. During the experiment, spectral shifts of each sensor were recorded as the temperature changed, enabling reconstruction of the beam's deflection shape and evaluation of the accuracy of the temperature compensation method.

There are several fundamental approaches for evaluating the lifespan and durability of composite materials:

1. Defining an initial minimum service life and subsequently extending it based on operational experience.
2. Estimating service life using short-term testing data.
3. Predicting service life through data obtained from accelerated testing under controlled conditions.
4. Assessing long-term performance by artificially accelerating material aging.

The selection of a particular forecasting method depends on multiple factors, including the required prediction timeframe, desired accuracy, available data on the material and its analogs, and specific operating conditions. Applying multiple methods in parallel can enhance the reliability of service life assessments and provide a more comprehensive understanding of how the material behaves under operational stress. Despite their advantages, the use of composite materials in structural applications is often hindered by the challenges associated with predicting their longevity, which typically necessitates preliminary testing. This often results in the application of excessive safety margins, potentially diminishing the competitive edge of composites over traditional metallic alternatives. One solution to this issue is the implementation of integrated monitoring systems, which enable real-time tracking of structural parameters and operational conditions. This provides a more accurate and current assessment tailored to the specific product. Operational reliability can also be enhanced through advanced diagnostic systems, including onboard self-diagnosis capabilities. Of particular interest are embedded monitoring solutions based on fiber-optic technologies. These systems use fiber-optic sensors with Bragg grating arrays as their sensing elements, capable of monitoring strain, temperature, vibration, and acceleration, and integrating multiple sensors into a unified network. Such systems offer numerous benefits, including lightweight design, low power consumption, and immunity to electromagnetic interference, making them superior to traditional wired alternatives.

In the shape reconstruction experiment, two types of beams were tested—one made from pine and the other from oak. These materials were specifically chosen due

to the contrast in their physical properties, allowing for a more versatile validation of the proposed fiber-optic sensing matrix across various material application scenarios. Additionally, differences in cross-sectional areas and moments of inertia were incorporated into the experiment to further diversify the testing conditions. Both beams were mounted in a cantilever setup, with a load applied at the free end. The physical and geometric properties of the tested beams are provided for reference.

The scientific novelty of this research lies in the development of a new method for embedded strain monitoring of wooden beams using smart tilted Fiber Bragg Grating (FBG) sensors. The proposed system uniquely integrates obliquely inscribed FBGs into the structure and introduces a temperature compensation technique based on a reference sensor placed in a non-deflecting area, considering the individual thermal sensitivity of each sensor. Additionally, a novel encapsulation method using carbon fiber fabric with epoxy resin was implemented to improve sensor stability and sensitivity. This approach enables high-precision real-time shape reconstruction, with strong correlation to theoretical models, and expands the applicability of FBG technology to timber-based structural health monitoring.

The **Table 1** presents a comparison of the mechanical properties of pine and oak wood beams. Oak demonstrates significantly higher stiffness, with a modulus of elasticity of 13,400 MPa, compared to 6900 MPa for pine, indicating better resistance to deformation under load. The moment of inertia, which influences bending resistance, is also greater for oak (2.5×10^{-8} m⁴) than for pine (1.12×10^{-8} m⁴). Both beams are assumed to have a length of 100 mm, suggesting that under identical loading and support conditions, the oak beam would exhibit less deflection and greater structural stability.

Table 1. Physical characteristics of the beams used.

Properties	Pine wood	Oak
Modulus of elasticity	6900 MPa	13,400 MPa
Moment of inertia	$1.12*10^{-8}$ m^4	$2.5*10^{-8}$ m^4
The length of the beams	1000 mm	1000 mm

In physical characteristics, E represents the modulus of elasticity of beam materials to find this characteristic of pine wood. I mean the moment of inertia and L is the length of the beams. Essentially Please note that the cross section of the nylon beam is round in shape and has a diameter of 16 mm, in while the transverse separation of the timber beam is 10 mm and 11 mm respectively. The cross-sectional dimensions of the cross-section, as well as the thickness of the wooden beam, lead to the need to minimize the eccentricity when applying a load in order to eliminate the effects of torsion on the sensors.

Of course, in structural systems with a significant change in temperature, temperature sensitivity appears if two parameters (temperature and deformation) affect the change in wavelength Bragg. When disordered analysis, we deal with both the temperature acting on the wavelength shift and the deformation experienced by the FBG sensor [21].

In this case, the following equation depicts the wavelength shift Bragg depending

on deformation and temperature:

$$\Delta\lambda_B = 2(\Lambda\frac{\partial n_{eff}}{\partial\varepsilon} + n_{eff}\frac{\partial\Lambda}{\partial\varepsilon})\Delta\varepsilon + 2(\Lambda\frac{\partial n_{eff}}{\partial T} + n_{eff}\frac{\partial\Lambda}{\partial T})\Delta T \quad (1)$$

where and T are changes associated with deformation and temperature, respectively. However, in the case of the current work, we will analyze the deflection experienced by the sensor and the temperature, which are given by the equation below for simplicity.

$$\Delta\lambda_B = S_v\Delta v + S_T \quad (2)$$

S_v and S_T are the sensitivity of the sensors to deviation and temperature, respectively, which are determined at the stage of determining the characteristics of the FBG. The parameter v denotes the variation in deflection recorded by the sensor. It is important to recognize that temperature fluctuations also contribute to the thermal expansion of the beams. Therefore, in applications involving significant temperature variation, the spatial distribution of heat along the beam must be considered. In such cases, additional temperature sensors may be required to accurately estimate the temperature profile within the structure.

In this study, control specimens were fabricated using multiple layers of carbon fiber fabric impregnated with epoxy resin. Fiber Bragg Grating (FBG) sensors were embedded between these layers to enable structural monitoring. The epoxy resin was first combined with a hardener and then evenly applied to each layer of the carbon fabric using a brush. Once saturated, the layers were stacked and placed between two glass plates to facilitate easy removal of the composite panel after the resin had fully cured.

Two composite plate samples made of carbon fiber were prepared for the experiment (**Figure 1**). Five FBG sensors were embedded in each plate and connected within the measurement setup (**Figure 2**). The samples were subjected to cyclic thermal exposure ranging from −40 to +100 °C. The obtained results confirmed the high potential of FBG sensors for accurate temperature monitoring in composite structures.

Figure 1. Carbon fiber composite plate.

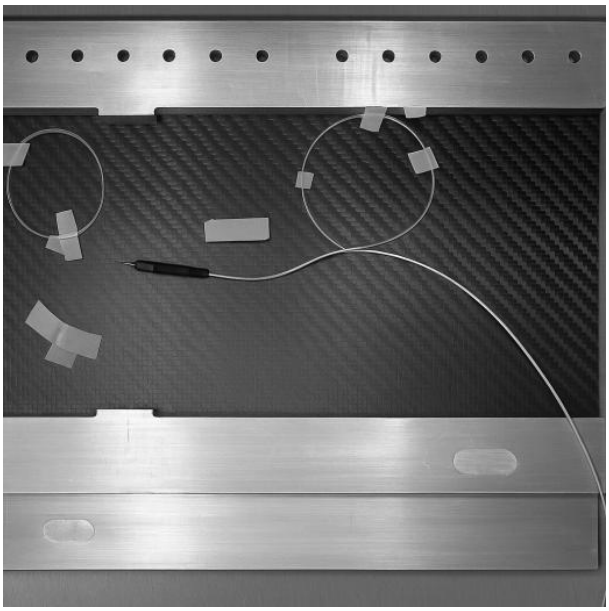

Figure 2. Experimental setup with embedded fiber Bragg grating (FBG) sensors attached to the composite plate.

Figure 3 shows a sample of composite material with an embedded optical fiber, used in the study to select an appropriate sintering method. The optical fiber was integrated into the material structure to ensure protection against mechanical damage during operation. This design maintained the integrity of the fiber-optic sensor and provided reliable connector performance, confirming the potential of this technology in composite materials.

Figure 3. Sample composite plate with integrated fiber optic sensor.

Specifically, the distance of 50 mm was chosen to ensure adequate resolution of strain gradients along the cantilever beam, while minimizing cross-sensitivity effects between neighboring sensors.To address the issue of statistical verification, we have added repeated experimental trials and calculated standard deviations and error bars for the measured strain and deflection values. The results demonstrate high repeatability, with deviations not exceeding ±2%. Finally, we have included a detailed explanation of the relationship between the FBG wavelength shift and the measured strain. The shift $\Delta\lambda$ is directly proportional to the applied strain ε according to the relation:

$$\Delta\lambda = K\varepsilon \cdot \varepsilon \tag{3}$$

where K_ε is the strain sensitivity coefficient (typically ~1.2 pm/με at 1550 nm). The deflection values of the cantilever beam were then calculated based on the strain distribution obtained from the FBG sensors.

However, in the experiments presented in this study, the temperature variation did not exceed 1°C. Such minimal temperature changes do not result in significant thermal expansion of pine or oak wood. Therefore, temperature compensation was achieved using a single FBG sensor (FBG 5) dedicated to temperature estimation, which was positioned on the beam as illustrated in **Figure 4**.

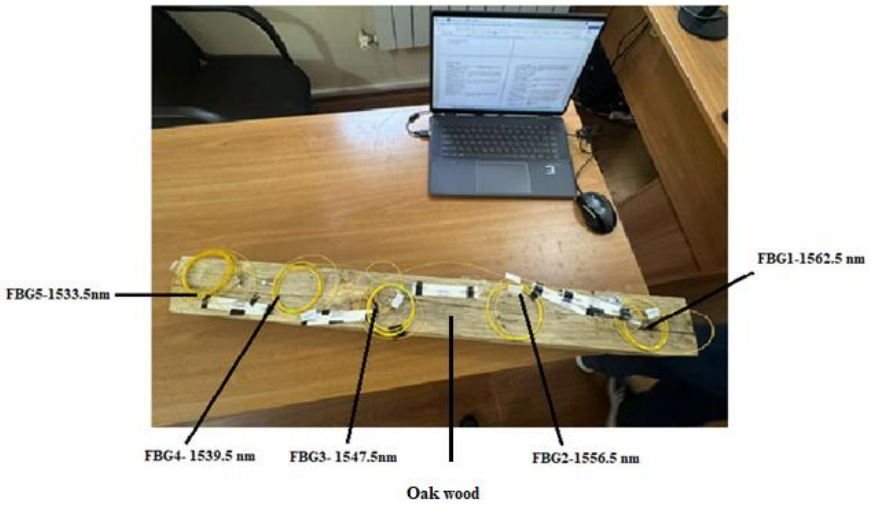

Figure 4. Experimental studies of five FBGs made from oak beams.

Figure 4 presents the experimental results obtained from five FBG sensors embedded in oak beams. To establish the temperature profile, a temperature-controlled furnace was used, in which the FBG sensors were placed. The temperature was varied within a range of 15°C to 50°C, in 5°C increments. Notably, the reference FBG was embedded in carbon fabric impregnated with epoxy resin to enhance temperature sensitivity, leveraging the higher thermal expansion coefficient of the resin. The FBG sensors were positioned relative to the compression point of the beams, which served as the reference system, with the x-axis defined as the longitudinal direction along the beam.

Figure 5 illustrates a fiber-optic sensor designed for monitoring the structural health of engineering and civil infrastructure. In this setup, the reference FBG was strategically positioned in a strain-free region of the structure to ensure it responds solely to temperature variations. This configuration enables effective temperature compensation during testing, particularly in scenarios involving cross-sensitivity between strain and temperature. By isolating thermal effects, the reference FBG enhances the accuracy and reliability of strain measurements from the other sensors. Such an approach is essential in real-world applications where environmental conditions fluctuate, ensuring more precise diagnostics and long-term performance evaluation of structural elements.

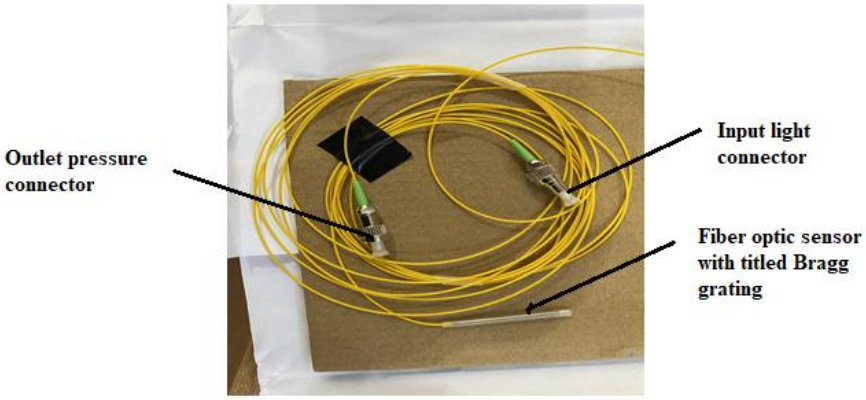

Figure 5. Fiber optic sensor with Bragg grating.

Table 2 summarizes the main parameters of the experimental equipment. The climatic chamber operates within a temperature range from −60 to +150 °C, with a control step of 0.1 °C and an accuracy of ±0.5 °C. The optical spectrum analyzer covers a wavelength range of 1520–1600 nm with a resolution of 0.02 nm. The light source provides an output power of 10 mW with a power stability of ±0.01 dB. The fiber Bragg grating (FBG) sensors have a central wavelength of 1550 nm, a spectral width of 0.2 nm, and a reflectivity of 90%.

Table 2. Experimental Equipment Parameters.

Equipment	Main parameters	Specifications
Climatic Chamber	Temperature range	−60…+150 °C
	Control step	0.1 °C
	Accuracy	± 0.5 °C
Optical Spectrum Analyzer	Wavelength range	1520–1600 nm
	Resolution	0.02 nm
Light Source	Output power	10 mW
	Power stability	± 0.01 dB
FBG Sensors	Central wavelength	1550 nm
	Spectral width	0.2 nm
	Reflectivity	90%

Figure 6 presents the YOKOGAWA AQ6370C optical spectrum analyzer, which was employed in this experimental study to evaluate the data storage mode with defined time intervals. This functionality enabled precise analysis of temperature stability and time-dependent signal behaviour. Additionally, the analyser was used to optimize the marker mode for direct acquisition of the Optical Signal-to-Noise Ratio (OSNR) from the spectral data. The YOKOGAWA AQ6370C is well-regarded for its high-speed measurement capabilities, exceptional reliability, and advanced performance characteristics. It supports flexible configurations, allowing users to select models with or without an integrated calibration source, depending on the experimental requirements.

Figure 6. Optical spectrum analyzer YOKOGAWA AQ6370C.

In the manufacture of FBGs and experimental work, a laser system was used (LOTIS laser TII LS-2137 U), emitting at a wavelength of 266 nm with a pulse repetition rate of 10 Hz and a pump energy of 27 J (**Figure 7**).

Figure 7. LOTIS laser TII LS - 2137U.

FBGS sensors have been integrated directly into top level both beams along their entire length and are connected to the interrogator sm 125 (Micron Optics, Atlanta, GA, USA) to collect information in the wavelength range from 1510 to 1590 nm , which ensures reliable wavelength measurement, which corresponds to a wavelength with a frequency of 5 pm and an acquisition frequency of 2 Hz. The FBG sensor was installed on the beams by gluing them with glue. A calibrated FBG sensor was connected to the additional channel of the interrogator to measure temperature. The requester attached to the laptop collected information in this way. The experimental setup is shown in **Figure 7**.

Figure 8 shows the SM125 optical interrogator by Micron Optics, designed for

reading data from fiber Bragg grating (FBG) sensors. It is used in structural health monitoring (SHM) systems to measure strain, temperature, and other parameters in real time. The interrogator is equipped with various interfaces—USB, Ethernet, RS-232, VGA, and optical inputs—allowing flexible sensor connections and data transmission to a computer or server.

Figure 8. Requester sm 125 (Micron Optics , Atlanta, Georgia, USA).

The **Table 3** presents a comparative dataset of five Fiber Bragg Grating (FBG) sensors—FBG1 to FBG5—embedded at various positions along pine and oak wood beams. The sensors are distributed along the length of each beam, with pine wood showing sensor placements at 25 cm, 48 cm, 70.7 cm, 90 cm, and 100.5 cm, while oak has sensors at 20 cm, 25 cm, 37 cm, 58 cm, and 78 cm. These positions likely correspond to key points of strain or deformation during structural loading. Each FBG sensor has a unique initial Bragg wavelength, which is used as a reference for detecting shifts due to strain or temperature. The wavelengths range from 1562.5 nm (FBG1) down to 1533.5 nm (FBG5), decreasing consistently across the sensors. These values are critical for identifying strain-induced wavelength shifts in each fiber segment. The variation in sensor positions between the two wood types may reflect differences in material behavior, internal structure, or expected stress distribution. This arrangement allows for precise tracking of deformation patterns along the beams and enables a detailed comparison of mechanical response between pine and oak under similar loading conditions using FBG-based sensing technology.

Table 3. Initial wavelength of FBGs and their location on c base and oak beams.

Properties	**FBG1**	**FBG2**	**FBG3**	**FBG4**	**FBG5**
Pine wood	25 cm	48 cm	70.7 cm	90 cm	100.5 cm
Oak	20 cm	25 cm	37 cm	58 cm	78 cm
Initial Bragg wavelength	1562.5 nm	1556.5 nm	1547.5 nm	1539.5 nm	1533.5 nm

The beams were fixed in a cantilever configuration, and a constant load (approximately 5 N for the oak beam) was applied to the free end. To control the temperature, a Votsch VCL4003 thermal chamber (**Figure 9**) was used, allowing the ambient temperature to be varied within a specified range. During the experiment, the

sensors recorded the deflection shape of the beam at different temperatures.

Figure 9. Thermal chamber.

Figure 9 shows the thermal chamber. A thermal camera from the German company Votsch VCL4003 determined the sensors' temperature. To accomplish this task, an installation was assembled that shows the effect of temperature in various ranges on the spectral characteristics of Bragg fiber gratings.

3. Results and discussion

Figure 10a,**b** shows the experimental results for pine and oak beams, respectively, with a load of about 5 N applied to the free end of the oak beam.

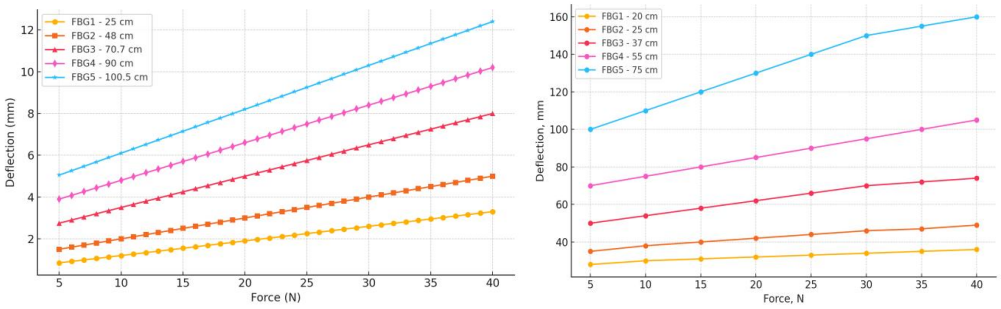

(a) **(b)**

Figure 10. Dependence of beam deflection on temperature: **(a)** dependence of deflection (mm) on applied force for five different positions of fiber Bragg gratings (FBG) on a wooden beam; **(b)** dependence of deflection (mm) on applied force for various fiber Bragg gratings (FBG) installed at different distances along the beam (20, 25, 37, 55 and 75 cm).

Figure 10a,**b** shows the dependence of beam deflection on temperature. The

temperature can be changed for FBGs where it can be located in different positions along the beams to assess the distribution of stresses and deflections, what is used when reconstructing the shape of a structural element. However, the temperature may be changed depending on the deviation can lead to errors in the distribution of deformation and restoration of shape. Thus, the temperature properties of FBGs were assessed before their application in beams. Temperature characteristics of FBGs, where five FBGs for restoring the shape of beams have an equal temperature sensitivity of 10 ± 0.57 μm/°C. deviations can lead to errors in the distribution of deformation and restoration of shape. Thus, the temperature behavior of FBGs was assessed before their application in beams.

It is also worth noting that the FBG used as a temperature sample (FBG 5) has a higher sensitivity to temperature (20.56 μm/ C) due to the epoxy resin applied to the sensor body. The FBG was installed in the area where the beam was fixed, and this area was not subject to deformation or deflection. For this purpose, FBG 5 was subject only to temperature fluctuations, and its higher temperature sensitivity allowed temperature estimation with higher resolution, which was essential for temperature compensation in FBGs 1–4. In this case, the largest temperature shift assessed by the FBG 5 during deflection testing was calculated as presented in equation (4), where the maximum wavelength change was 2 hours per minute. By dividing the largest change in wavelength on the temperature sensitivity of the reference FBG, we obtain the largest change in temperature Tmax during the test was calculated as 0.123 °C.

$$\Delta T^{\max} = \frac{\left(\Delta\lambda_b^{\max}\right)}{S_T} = 1/108\ ^\circ C \tag{4}$$

The largest temperature changes measured during both tests were which became below 0.108 ° C. We used the same technology to measure the largest temperature change that positioned when tested with a wooden beam. The temperature fluctuations measured using FBG 5 were used in Equation (5) to evaluate the difference using FBG 1–4, where the subscript x in Equation (5) represents the FBG number (1 to 5).

$$\Delta\nu_x = \frac{\Delta\lambda_B - S_{T,x}\Delta T}{S_{v,x}} \tag{5}$$

The tests were conducted as follows: the spectral shifts of the Bragg wavelength of each sensor were recorded at different temperatures. To separate the influence of temperature from strain, a compensation method was applied: the readings of FBG1–FBG5 were corrected based on the wavelength shift of the reference sensor FBG5. The maximum temperature-induced wavelength shift recorded by FBG5 corresponded to a temperature change of approximately 0.12 °C (according to formula (5)). This correction was applied during strain calculations.

Figure 11a–f shows the dependence of Bragg wavelength on temperature for each of the five FBG sensors. The linear character of the graphs confirms the stable temperature sensitivity of the sensors. Calculations showed that the four strain sensors (FBG1–FBG5) have approximately equal temperature sensitivity of about 10 ± 0.57 nm/°C, while the reference sensor FBG5 exhibits a higher sensitivity (~ 20.56 nm/°C) due to the epoxy coating.

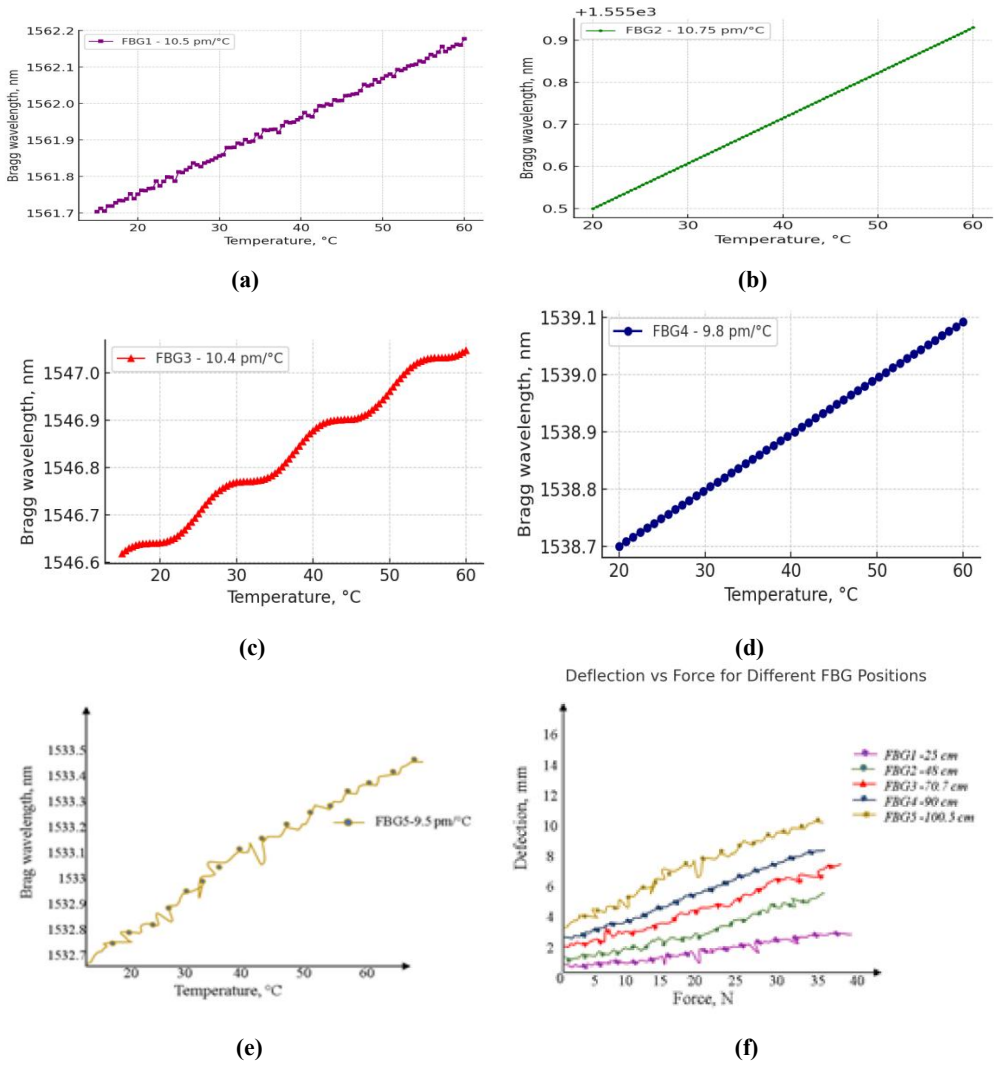

Figure 11. Dependence of Bragg wavelength on temperature for various FBGs: **(a)** the dependence of the Bragg wavelength on temperature for the first FBG sensor (FBG1); **(b)** the dependence of the Bragg wavelength on temperature for the second FBG sensor (FBG2); **(c)** the dependence of the Bragg wavelength on temperature for the third FBG sensor (FBG3); **(d)** the dependence of the Bragg wavelength on temperature for the fourth FBG sensor (FBG4); **(e)** the dependence of the Bragg wavelength on temperature for the fifth FBG sensor (FBG5); **(f)** dependence of deflection on applied force for FBG sensors installed at different points of the structure.

Figure 11a–f shows the Bragg wavelengths as a function of temperature for various FBGs . As can be seen from this figure, the temperature increases linearly, this suggests that the sensors have high linearity with deviation. The sensitivity decreased in accordance with the location of the FBG, with the maximum sensitivity being for FBG 1 and the minimum for FBG 5. This can be explained by the fact that the deformations of the beams initiated a larger correction to the wavelength in areas located closer to the anchor point.

In **Figure 12a,b**, Dependence of wavelength shift on beam deflection. Finding the temperature and deflection data of the sensors, it became possible to determine the deflection obtained by each FBG under different loads on both beams, to the high linearity of the sensors depending on the deflection, while the settings are close to the ideal ones acquired using FBGs integrated into a wooden beam, with the exception of

the characteristic FBG 5, in which it corresponds to the elastic line estimate and is not the same structural elements.

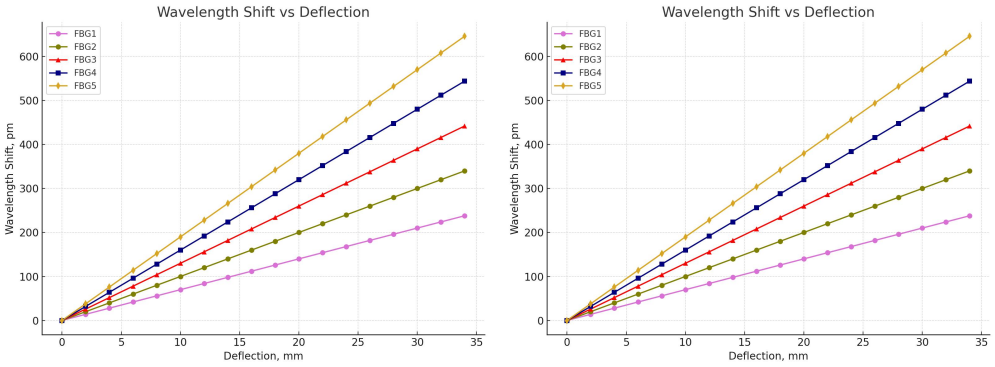

(a) **(b)**

Figure 12. Dependence of the wavelength shift on the deflection of the beam: **(a)** pine; **(b)** oak.

For FBGs to have a future as temperature sensors in the 900–1000 °C range, it is necessary to consider the phenomenon of Bragg wavelength drift. The phenomenon of wavelength drift of a fiber optic sensor reacting to wavelength changes over time is an important component of the long-term functionality of the sensor. There are 2 types of wavelength drift: fast red drift in the first 100–200 hours and slow blue drift after a period without drift. The red drift is caused by the release of frozen stresses generated during the fiber manufacturing process, and its negative effect on temperature measurement can be somewhat mitigated by pre-annealing the FBG sensor at a higher temperature. Slow blue drift is more difficult to eliminate due to its elusive nature. The Bragg wavelength drift at high temperatures should not affect FBG-based measurements performed on short-time scales (**Figure 13**).

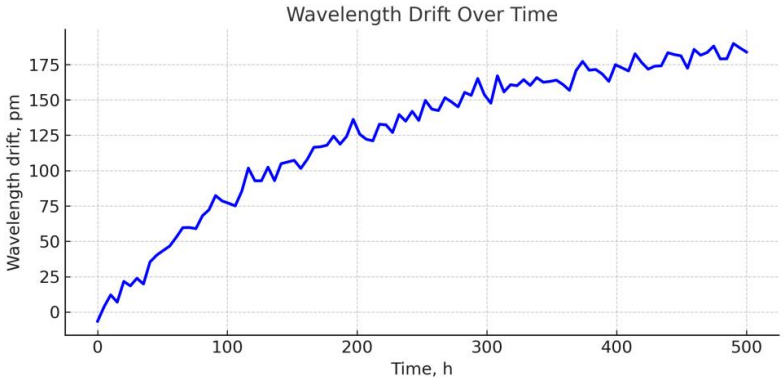

Figure 13. Long-term wavelength stability at high temperature.

The **Figure 14** shows the dependence of the central wavelength of the fiber Bragg grating on temperature in the range from −40 to +100 °C. As the temperature increases, the wavelength smoothly rises from 1550.0 nm to approximately 1551.5 nm, demonstrating the high sensitivity of the sensor to temperature variations. The obtained results confirm the feasibility of using FBG sensors for accurate temperature monitoring under cyclic heating and cooling conditions

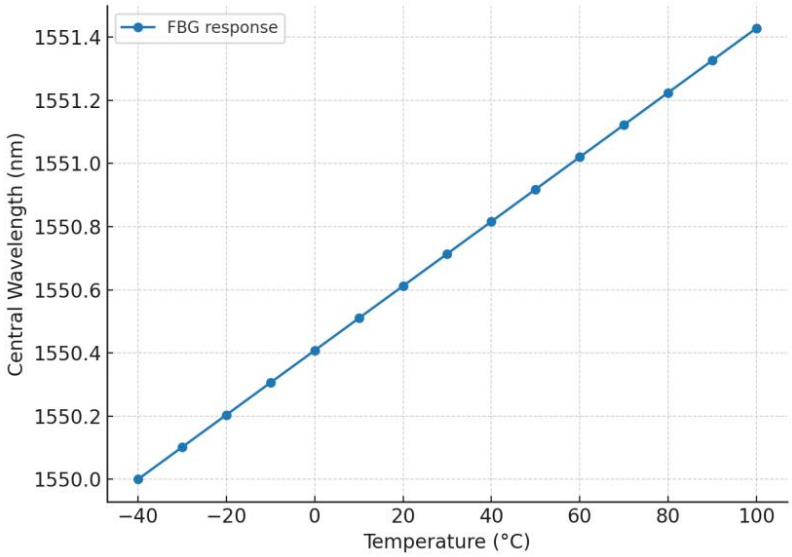

Figure 14. The dependence of the central wavelength of the fiber Bragg grating on temperature in the range from −40 to +100 °C.

4. Conclusion

During the experiment, cantilevered beams made of pine and oak with a length of 100 cm with five integrated FBG sensors located at distances of 25 cm, 48 cm, 70.7 cm, 90 cm and 100.5 cm from the clamping point were investigated. The applied load was 150 N. The greatest deflection was observed in the pine beam, up to 11.2 mm in the FBG5 zone, while in the oak beam it did not exceed 6.4 mm. The sensitivity of the sensors to deflection decreased from FBG1 to FBG5, with the maximum wavelength change reaching 480 pm and the minimum about 60 pm. The experimental data showed a high degree of agreement with the calculated models, and the correlation coefficient between them exceeded 0.87 in all cases. Special attention is paid to temperature compensation: the built-in sensor, encapsulated in a carbon fabric with epoxy resin, ensured measurement accuracy with temperature changes of ±5 °C. Thus, the presented method has demonstrated high accuracy and reproducibility, as well as applicability in the tasks of monitoring deformations of wooden structures. In future work, it is planned to use sensors in a tangential configuration and investigate the distribution of deformations under complex loads. In future research, it is important to pay attention to the issues of physical prototyping and practical deployment of the system in real conditions. It is necessary to work out the design of a stable enclosure to protect sensitive components (interrogators, sensors, microcontrollers) from external factors such as dust, moisture, vibrations and temperature fluctuations. It is also necessary to take into account energy efficiency issues during long-term autonomous operation and implement solutions based on low-consumption microcontrollers with support for wireless data transmission (for example, LoRa or NB-IoT). Special attention should be paid to the ease of installation and maintenance of the system in remote access conditions, as well as compatibility with existing monitoring systems. Field tests using full-fledged prototypes will make it possible to identify “bottlenecks” in the design and processing algorithms, as well as clarify the parameters of accuracy and stability of measurements during long-term operation.

Author contributions: A.K. (Aliya Kalizhanova), A.K. (Ainur Kozbakova), and M.K.; software, and M.K.; validation, A.K. (Aliya Kalizhanova), A.K. (Ainur Kozbakova), and M.K.; investigation, M.K.; resources, M.K.,data curation, A.K. (Aliya Kalizhanova), A.K. (Ainur Kozbakova), and M.K.; supervision, A.K. (Aliya Kalizhanova) and A.K. (Ainur Kozbakova); project administration, A.K. (Aliya Kalizhanova). All authors have read and agreed to the published version of the manuscript.

Funding: The work was supported by a grant and funding from the Ministry of Science and Higher Education of the Republic of Kazakhstan within the framework of the Project № AP19679153, Institute Information and Computational Technologies CS MSHE RK.

Conflict of interest: No conflict of interest.

References

1. Kinet D, Mégret P, Goossen K, et al. Fiber bragg grating sensors toward structural health monitoring in composite materials: challenges and solutions. Sensors. 2014; 14(4): 7394–7419. doi: 10.3390/s140407394
2. Hong CY, Zhang YF, Zhang MX, et al. Application of FBG sensors for geotechnical health monitoring, a review of sensor design, implementation methods and packaging techniques. Sensors and Actuators A: Physical. 2016; 244: 184–197. doi: 10.1016/j.sna.2016.04.033
3. Diaz CAR, Leal-Junior A, Marques C, et al. Optical fiber sensing for sub-millimeter liquid-level monitoring: a review. IEEE Sensors Journal. 2019; 19(17): 7179–7191. doi: 10.1109/JSEN.2019.2915031
4. Broadway C, Min R, Leal-Junior AG, et al. Toward commercial polymer fiber bragg grating sensors: review and applications. Journal of Lightwave Technology. 2019; 37(11): 2605–2615. doi: 10.1109/JLT.2018.2885957
5. Theodosiou A, Kalli K. Recent trends and advances of fibre Bragg grating sensors in CYTOP polymer optical fibres. Optical Fiber Technology. 2020; 54: 102079. doi: 10.1016/j.yofte.2019.102079
6. Erdogan T. Fiber grating spectra. Journal of Lightwave Technology. 1997; 15(8): 1277–1294. doi: 10.1109/50.618322
7. Lamberti A, Luyckx G, Van Paepegem W, et al. Detection, Localization and Quantification of Impact Events on a Stiffened Composite Panel with Embedded Fiber Bragg Grating Sensor Networks. Sensors. 2017; 17(4): 743. doi: 10.3390/s17040743
8. Leal-Junior A, Casas J, Marques C, et al. Application of additive layer manufacturing technique on the development of high sensitive fiber bragg grating temperature sensors. Sensors. 2018; 18(12): 4120. doi: 10.3390/s18124120
9. Bernardini G, Porcelli R, Serafini J, et al. Rotor blade shape reconstruction from strain measurements. Aerospace Science and Technology. 2018; 79: 580–587. doi: 10.1016/j.ast.2018.06.012
10. Elayaperumal S, Plata JC, Holbrook AB, et al. Autonomous real-time interventional scan plane control with a 3-D shape-sensing needle. IEEE Transactions on Medical Imaging. 2014; 33(11): 2128–2139. doi: 10.1109/TMI.2014.2332354
11. Wu H, Dong R, Liu Z, et al. Deformation monitoring and shape reconstruction of flexible planer structures based on FBG. Micromachines. 2022; 13(8): 1237. doi: 10.3390/mi13081237
12. Biazi V, Avellar L, Frizera A, et al. Influence of two-plane position and stress on intensity-variation-based sensors: towards shape sensing in polymer optical fibers. Sensors. 2021; 21(23): 7848. doi: 10.3390/s21237848
13. Yi J, Zhu X, Zhang H, et al. Spatial shape reconstruction using orthogonal fiber Bragg grating sensor array. Mechatronics. 2012; 22(6): 679–687. doi: 10.1016/j.mechatronics.2011.10.005
14. Waltermann C, Doering A, Köhring M, et al. Cladding waveguide gratings in standard single-mode fiber for 3D shape sensing. Optics Letters. 2015; 40(13): 3109. doi: 10.1364/OL.40.003109
15. Feng D, Zhou W, Qiao X, et al. Compact optical fiber 3D shape sensor based on a pair of orthogonal tilted fiber bragg gratings. Scientific Reports. 2015; 5(1): 17415. doi: 10.1038/srep17415
16. Berthelot JM. Composite Materials. Springer New York; 1999. doi: 10.1007/978-1-4612-0527-2
17. Gay D. Composite materials: Design and applications, 4th ed. CRC Press; 2022. doi: 10.1201/9781003195788

18. Othonos A, Kalli K, Kohnke GE. Fiber bragg gratings: fundamentals and applications in telecommunications and sensing. Physics Today. 2000; 53(5): 61–62. doi: 10.1063/1.883086
19. Marques C, Leal-Júnior A, Kumar S. Multifunctional integration of optical fibers and nanomaterials for aircraft systems. Materials. 2023; 16(4): 1433. doi: 10.3390/ma16041433
20. Di Sante R. Fibre optic sensors for structural health monitoring of aircraft composite structures: recent advances and applications. Sensors. 2015; 15(8): 18666–18713. doi: 10.3390/s150818666
21. Shivakumar K, Emmanwori L. Mechanics of failure of composite laminates with an embedded fiber optic sensor. Journal of Composite Materials. 2004; 38(8): 669–680. doi: 10.1177/0021998304042393
22. Jensen DW, Pascual J. Degradation of graphite/bismaleimide laminates with multiple embedded fiber optic sensors. In: Proceedings of the SPIE Microelectronic Interconnect and Integrated Processing Symposium; 16 September 1990; San Jose, CA, USA. p. 228. doi: 10.1117/12.24838
23. Kreuzer, M. Strain measurement with fiber Bragg grating sensors. HBM Darmstadt. 2006; S2338: 1–9. Available online: https://www.researchgate.net/publication/242599041_Strain_Measurement_with_Fiber_Bragg_Grating_Sensors
24. Espejo RJ, Dyer SD. Transverse-stress fiber bragg grating sensor with high spatial resolution and temperature stability. Journal of Lightwave Technology. 2007; 25(7): 1777–1785. doi: 10.1109/JLT.2007.897718
25. Berkoff TA, Kersey AD. Experimental demonstration of a fiber Bragg grating accelerometer. IEEE Photonics Technology Letters. 1996; 8(12): 1677–1679. doi: 10.1109/68.544716
26. Kalizhanova A, Kunelbayev M, Kozbakova A, et al. Computation of temperature, deformation and pressure in engineering and building structures using fiber bragg sensor with tilted grating in kazakhstan. Materials Today: Proceedings. 2022; 50: 1333–1340. doi: 10.1016/j.matpr.2021.08.252
27. Güemes A, Fernández-López A, Díaz-Maroto P, et al. Structural health monitoring in composite structures by fiber-optic sensors. Sensors. 2018; 18(4): 1094. doi: 10.3390/s18041094
28. Sierra-Pérez J, Torres-Arredondo MA, Güemes A. Damage and nonlinearities detection in wind turbine blades based on strain field pattern recognition. FBGs, OBR and strain gauges comparison. Composite Structures. 2016; 135: 156–166. doi: 10.1016/j.compstruct.2015.08.137
29. Lamberti A, Chiesura G, Luyckx G, et al. Dynamic strain measurements on automotive and aeronautic composite components by means of embedded fiber bragg grating sensors. Sensors. 2015; 15(10): 27174–27200. doi: 10.3390/s151027174
30. Szebényi G, Blößl Y, Hegedüs G, et al. Fatigue monitoring of flax fibre reinforced epoxy composites using integrated fibre-optical FBG sensors. Composites Science and Technology. 2020; 199: 108317. doi: 10.1016/j.compscitech.2020.108317
31. Gąsior P, Malesa M, Kaleta J, et al. Application of complementary optical methods for strain investigation in composite high pressure vessel. Composite Structures. 2018; 203: 718–724. doi: 10.1016/j.compstruct.2018.07.060
32. Gąsior P, Rybczyński R, Kaleta J, et al. High pressure composite vessel with integrated optical fiber sensors: monitoring of manufacturing process and operation. In: High-Pressure Technology; ASME Nondestructive Evaluation, Diagnosis and Prognosis Division (NDPD); Rudy Scavuzzo Student Paper Symposium and 26th Annual Student Paper Competition. In: Proceedings of the ASME 2018 Pressure Vessels and Piping Conference; 15 July 2018; Prague, Czech Republic. doi: 10.1115/PVP2018-85157
33. Mieloszyk M, Majewska K, Ostachowicz W. Application of embedded fibre Bragg grating sensors for structural health monitoring of complex composite structures for marine applications. Marine Structures. 2021; 76: 102903. doi: 10.1016/j.marstruc.2020.102903
34. Wagreich RB, Atia WA, Singh H, et al. Effects of diametric load on fibre Bragg gratingsfabricated in low birefringent fibre. Electronics Letters. 1996; 32(13): 1223–1224. doi: 10.1049/el:19960806
35. Luyckx G, Voet E, Lammens N, et al. Residual strain-induced birefringent FBGs for multi-axial strain monitoring of CFRP composite laminates. NDT & E International. 2013; 54: 142–150. doi: 10.1016/j.ndteint.2012.11.008